

The Icelandic Low as a Predictor of the Gulf Stream North Wall Position

ALEJANDRA SANCHEZ-FRANKS

National Oceanography Centre, Southampton, United Kingdom

SULTAN HAMEED AND ROBERT E. WILSON

School of Marine and Atmospheric Sciences, Stony Brook University, Stony Brook, New York

(Manuscript received 24 November 2014, in final form 6 November 2015)

ABSTRACT

The Gulf Stream's north wall east of Cape Hatteras marks the abrupt change in velocity and water properties between the slope sea to the north and the Gulf Stream itself. An index of the north wall position constructed by Taylor and Stephens, called Gulf Stream north wall (GSNW), is analyzed in terms of interannual changes in the Icelandic low (IL) pressure anomaly and longitudinal displacement. Sea surface temperature (SST) composites suggest that when IL pressure is anomalously low, there are lower temperatures in the Labrador Sea and south of the Grand Banks. Two years later, warm SST anomalies are seen over the Northern Recirculation Gyre and a northward shift in the GSNW occurs. Similar changes in SSTs occur during winters in which the IL is anomalously west, resulting in a northward displacement of the GSNW 3 years later. Although time lags of 2 and 3 years between the IL and the GSNW are used in the calculations, it is shown that lags with respect to each atmospheric variable are statistically significant at the 5% level over a range of years. Utilizing the appropriate time lags between the GSNW index and the IL pressure and longitude, as well as the Southern Oscillation index, a regression prediction scheme is developed for forecasting the GSNW with a lead time of 1 year. This scheme, which uses only prior information, was used to forecast the GSNW from 1994 to 2015. The correlation between the observed and forecasted values for 1994–2014 was 0.60, significant at the 1% level. The predicted value for 2015 indicates a small northward shift of the GSNW from its 2014 position.

1. Introduction

Labrador Sea Water (LSW), formed in convective processes in the Labrador Sea, makes up the upper component of the deep western boundary current in the North Atlantic. The deep western boundary current crosses under the Gulf Stream near 36°N, an important region of interaction between the two different water masses. Hydrographic and tracer surveys of the crossover region show that a part of the LSW transported by the deep western boundary current turns away from the shore at the crossover and becomes incorporated with the northern part of the Gulf Stream (Pickart and Smethie 1993; Bower and Hunt 2000). At the northern edge of the Gulf Stream, where its warm waters meet the cold Labrador Sea–derived flow, a

sharp temperature gradient known as the Gulf Stream north wall (GSNW) is created. Interannual fluctuations of the latitude at which the GSNW occurs are associated with changes in sea surface temperature (SST) distribution northward and thus with regional climate and plankton distributions.

The analysis presented in this paper is based on the GSNW index of Taylor and Stephens (1980, 1998). This index has been used in studies of plankton abundance in the eastern North Atlantic, the North Sea (Taylor 1995; Planque and Taylor 1998), Narragansett Bay (Borkman and Smayda 2009), and lakes in Ireland (Jennings and Allott 2006). From current measurements in the slope sea, Bane et al. (1988) found the southwestward shelf-break current is stronger when the Gulf Stream is located more to the north and closer onshore, and it is weaker when the Gulf Stream is situated farther south, offshore. They suggested that this relationship is driven by the Gulf Stream's impact on the Northern Recirculation Gyre from both its shift in position and the shedding of warm core rings. Following Csanady and

Corresponding author address: Sultan Hameed, School of Marine and Atmospheric Sciences, Stony Brook University, 125 Endeavour Hall, Stony Brook, NY 11794-5000.
E-mail: sultan.hameed@stonybrook.edu

Hamilton (1988), the slope sea is defined here as the region of ocean located between the continental shelf and the Gulf Stream, extending from Cape Hatteras to the tail of the Grand Banks.

Taylor and Stephens (1998) also showed that the GSNW is significantly correlated to the North Atlantic Oscillation (NAO). They presented a regression model of the GSNW using a 1-yr lagged GSNW and a 2-yr lagged NAO index. In this scheme, southward (northward) anomalies of the GSNW latitude are associated with a low (high) NAO phase. Taylor et al. (1998) showed that more of the GSNW's variability could be explained when the Southern Oscillation index (SOI), lagged 2 years, was added as an independent variable in the regression equation. They found that, for 1966–97, 60% of the GSNW's variance was explained using the GSNW (lagged 1 year) and the NAO (lagged 2 years); another 9% was explained by the SOI, also lagged 2 years. Later, Hameed and Piontkovski (2004) discovered that the variance of the GSNW explained in the regression model of Taylor and Stephens (1998) increased significantly when the NAO was decoupled into its component centers of action, the Icelandic low (IL) and the Azores high (AH), characterized by their pressure, latitude, and longitude. Their regression model was dominated by the IL pressure (lagged 2 years) and IL longitude (lagged 3 years). The direct contribution, or partial correlation coefficient, of the AH to the variation of the GSNW was insignificant. Because the northerly winds around the IL cause cooling in the Labrador Sea, their results suggested that variations in the southward flow of LSW are an important influence on the GSNW position.

This paper has a threefold purpose. First, we report that the relationship between the GSNW and the IL pressure and longitude position described by Hameed and Piontkovski (2004) has been maintained up to present. Second, we examine SST anomalies in the North Atlantic for winters when the IL pressure is anomalously low (high), and for winters in which the IL longitude has shifted anomalously west (east). These anomalies are indicative of dynamical changes in the ocean consequent to changes in wind stress and heat fluxes that accompany the fluctuations in the strength and position of the IL. A third purpose of this paper is to show that GSNW can be forecasted at least 1 year in advance. Noting that the GSNW is correlated with IL pressure and longitude position and the SOI, each with a 2–3-yr lag, we develop a statistical model for predicting GSNW position with a lead time of 1 year, using only prior information. This is used to make 1- and 2-yr-forward forecasts of GSNW position for each year from 1994 to 2015.

2. Update of relationship between the Icelandic low and the Gulf Stream north wall

The GSNW dataset used here is the index computed by Taylor and Stephens (1980) from the first principal component of the position of the north wall's latitude from six different longitudes: 79°, 75°, 72°, 70°, 67°, and 65°W. The temperature measurements used to identify the Gulf Stream position have been collected since 1966 by the U.S. Naval Oceanographic Office, NOAA, the Oceanographic Monthly Summary, and the U.S. Navy. (Both monthly and annual means are available at <http://www.pml-gulfstream.org.uk/default.htm>.) To maintain continuity with previous studies of the GSNW, this paper uses only annual means of the index.

The second dataset used was the IL pressure and longitude indices, constructed from gridded NCEP–NCAR reanalysis monthly sea level pressure (SLP) data (Kalnay et al. 1996) as described by Hameed and Piontkovski (2004). Objective indices for the IL are calculated by using the air mass distribution over its domain. By examining the monthly SLP maps over the North Atlantic since 1900, the latitude–longitude domain of the IL was chosen as 40°–75°N, 90°W–20°E. The monthly averaged pressure of the IL is then estimated as the area-weighted mean pressure over all the grid points in the domain where the pressure is less than a threshold value of 1014 mb. The longitude position index is defined as the pressure-weighted longitudinal location of the centroid of the air mass over the grid points where the pressure is less than the threshold value. Further details on the calculation of the indices are given by Hameed and Piontkovski (2004).

Hameed and Piontkovski (2004) investigated the relationship between the GSNW and the NAO for the years 1966–2000. By decoupling the NAO into the IL and the AH, they found that the largest correlations with the GSNW were with the IL pressure lagged 2 years and the IL longitude lagged 3 years. The first two rows of Table 1 give the statistics of these correlations for the 1966–2000 years. We have updated these results for 1966–2014 (bottom two rows of Table 1) and find the lagged correlations between GSNW and IL pressure and longitude have stayed robust through the longer period. Since GSNW and IL pressure and longitude have significant autocorrelations, the effective sample size n' for the correlations was estimated using the method of Quenouille (1953) as

$$n' = n / (1 + 2r_1r'_1 + 2r_2r'_2 + 2r_3r'_3 + \dots),$$

where n is the number of data in each series, r_1 and r'_1 are the autocorrelations at lag 1 in the two data series, r_2 and r'_2 the autocorrelations at lag 2, etc.

TABLE 1. The sample size n , the effective sample size n' , and the correlation coefficient r between the GSNW and IL pressure (lagged 2 years), and longitude position (lagged 3 years) compared between the 1966–2000 and 1966–2014 periods. All correlation coefficients are statistically significant at the 1% level.

Variable	n	n'	r
IL pressure 1966–2000	35	21	−0.59
IL longitude 1966–2000	35	25	−0.50
IL pressure 1966–2014	49	30	−0.52
IL longitude 1966–2014	49	37	−0.40

3. Time lags between changes in the IL and the GSNW

There are multiple intraseasonal and interannual time scales for variations in the IL pressure and position. Similarly, there are multiple time scales that influence the western boundary current. As a result the time lags between the changes in the IL and changes in GSNW vary over a range of years. Hameed and Piontkovski (2004) showed correlations with lags of 0–5 years in their Table 1, where it was seen that the correlations between IL pressure and GSNW were statistically significant for lags of 0, 1, and 2 years, and for IL longitude the correlations for 3- and 4-yr lags were statistically significant. However, the percentage of GSNW variance explained was maximized for a 2-yr lag for IL pressure and a 3-yr lag for IL longitude. The lags at which the correlations are statistically significant for the extended data, 1966–2014, are shown in Table 2, where we again see that the correlations of GSNW and IL pressure are significant for lags of 0, 1, and 2 years and those for IL longitude are significant for lags of 3 and 4 years at the 5% level. The table shows the interesting result that the correlation between the NAO and GSNW is statistically significant for lags of 0, 1, and 2 years. The highest correlation is at a lag of 1 year, although a lag of 2 years with respect to the NAO was used in the regression model of Taylor and Stephens (1998). Table 2 also indicates that the correlation between the SOI and the GSNW is statistically significant with only the lag of 2 years. The physical mechanism that would explain this relationship between El Niño–Southern Oscillation and GSNW remains unidentified.

Bower and Hunt (2000) deployed floats at the levels of upper LSW (800 m) and overflow water (3000 m) in the deep western boundary current between the Grand Banks and Cape Hatteras to measure the spreading rates of these two water masses. They estimated mean advection velocities along the upper LSW as 2–4 cm s^{−1}. These estimates translate to a travel time of 2–4 years for a water parcel to travel the 1700 km between the Grand Banks and Cape Hatteras, consistent with the

TABLE 2. Correlation between the GSNW and the atmospheric variables with lags from 0 to 5 years. Results in bold indicate the correlation coefficient is significant at the 5% level.

Variable/lag	0	1	2	3	4	5
NAO	0.46	0.52	0.39	0.16	0.08	0.18
IL pressure	−0.40	−0.40	−0.52	−0.22	−0.19	−0.26
IL longitude	−0.01	0.07	−0.01	−0.40	−0.42	−0.21
SOI	−0.08	0.10	−0.29	−0.08	−0.02	−0.08

multiyear lag times between the IL and the GSNW shown in Table 2.

Using a combination of altimetric and hydrographic (CTD) data, Han et al. (2010) measured Labrador Current transport between the 600- and 3400-m isobaths in the Labrador Sea north of the Hamilton Bank (56°N) over 1993–2004. They found the multiyear changes in the Labrador Current transport to be primarily barotropic and positively correlated with the NAO at zero lag. This suggests Labrador Sea circulation responds to atmospheric variability within a year.

4. SST response to IL variations

In this section, relationships between IL pressure and longitudinal position and the distribution of SST in the North Atlantic are examined. NOAA Optimum Interpolated (OI) SST version 2 data available from 1981 to 2012 with a 1° × 1° resolution are used for the SST composites. The SST data may be found on NOAA's physical sciences division website (<http://www.esrl.noaa.gov/psd/data/gridded/data.noaa.oisst.v2.html>).

Figure 1a shows a composite of SST anomalies during 1981–2012 in winters [December–February (DJF)] for which the area-averaged IL pressure was more than one standard deviation lower than its mean value (1989, 1990, 1995, and 2007). Cold anomalies of −0.1° to −1.0°C extend from the mouth of the Labrador Sea to the southeast and east of Greenland and southward of the Grand Banks and the Scotian Shelf, as would be expected from the impact of intensified cyclonic winds that accompany very low IL pressures. Figure 1b shows SST anomalies 2 years later, that is, winters with a 2-yr lag with respect to those shown in Fig. 1a, where the cold SST anomalies south of the Grand Banks, observed 2 years prior, have been replaced by warm SSTs in the range of 0.2°–1.0°C, suggesting a northward shift of the GSNW. Warm anomalies in the slope sea were attributed by Rossby and Benway (2000) to a reduction of cold water flux from the Labrador shelf, consistent with the warm temperature anomalies south of the Grand Banks in Fig. 1b. We note the cold SST anomaly in the Gulf of Maine is not consistent with this picture. An

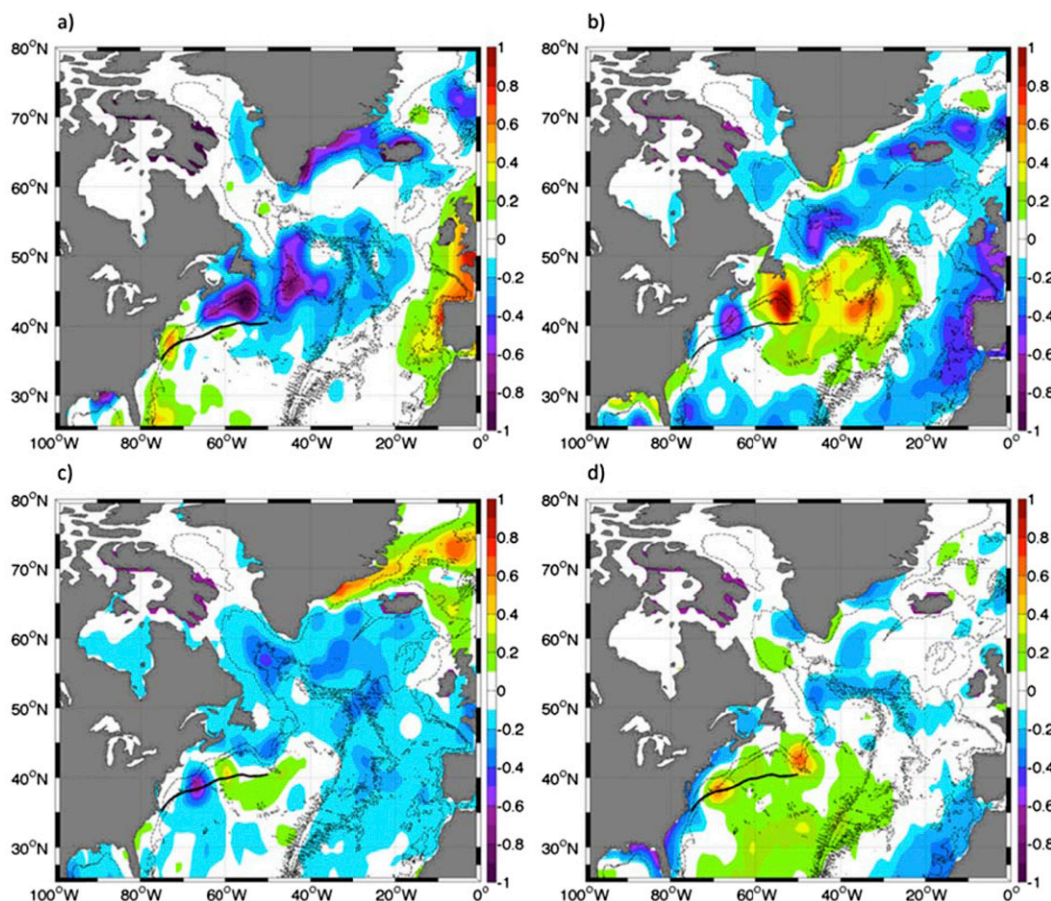


FIG. 1. Winter (DJF) composite SST anomalies ($^{\circ}\text{C}$) for the time range 1981–2012. Shown for the IL pressure during its lowest years (a) with no lag and (b) with a 2-yr lag and the IL longitude during its westernmost years (c) with no lag and (d) with a 3-yr lag. The mean Gulf Stream path is superimposed (black line) on the SST anomalies. The winter average for a particular winter is the average of the December value of the previous year and January and February values of the current year. The thin lines represent the 1000- and 3500-m isobaths.

estimate of the mean Gulf Stream path is superposed (black line) on the SST in all panels of Fig. 1 using the Canadian marine environmental data service (MEDS). The MEDS mean Gulf Stream position is estimated from SST anomalies at every degree longitude between 75° and 50°W .

Figure 1c depicts composite SST anomalies in the winters when the IL longitude was displaced westward by more than one standard deviation of its mean longitudinal position (1985, 1987, 1991, 1992, 1996, 2003, and 2006). Cold SST anomalies of -0.2° to -0.5°C are seen in the Labrador Sea, extending eastward and southward to the Grand Banks and the Scotian Shelf and to the eastern side of the North Atlantic. Figure 1d shows the composite SST anomalies 3 years after those shown in Fig. 1c, that is, lagged 3 years with respect to extreme westward positioning of the IL, as is suggested by the correlation calculations (Table 2). SST anomalies in

Fig. 1d are warmer south of the Grand Banks and Scotian Shelf in comparison with the anomalously west IL longitude (Fig. 1c), indicating a reduction in the spilling of cold waters from the north into the slope sea, as hypothesized by Rossby and Benway (2000).

Analogous to the anomalously low and anomalously west IL pressures in Fig. 1, anomalously high and anomalously east IL pressures are considered in Fig. 2. Figure 2a shows winter SST anomaly composites for anomalously high IL pressures (1996, 2001, 2004, 2006, 2010, and 2011) at zero-year lag. Warm anomalies of 0.5° to 1.0°C are observed in the Labrador Sea, east of Newfoundland, and in the Gulf of St. Lawrence, and cool anomalies of -0.3° to -1.0°C are apparent along the U.S. eastern seaboard (Fig. 2a). Contrary to the SST structure depicted in the anomalously low IL pressure years (Fig. 1a), during anomalously high IL pressure winters, the IL pressure system is decreased in strength

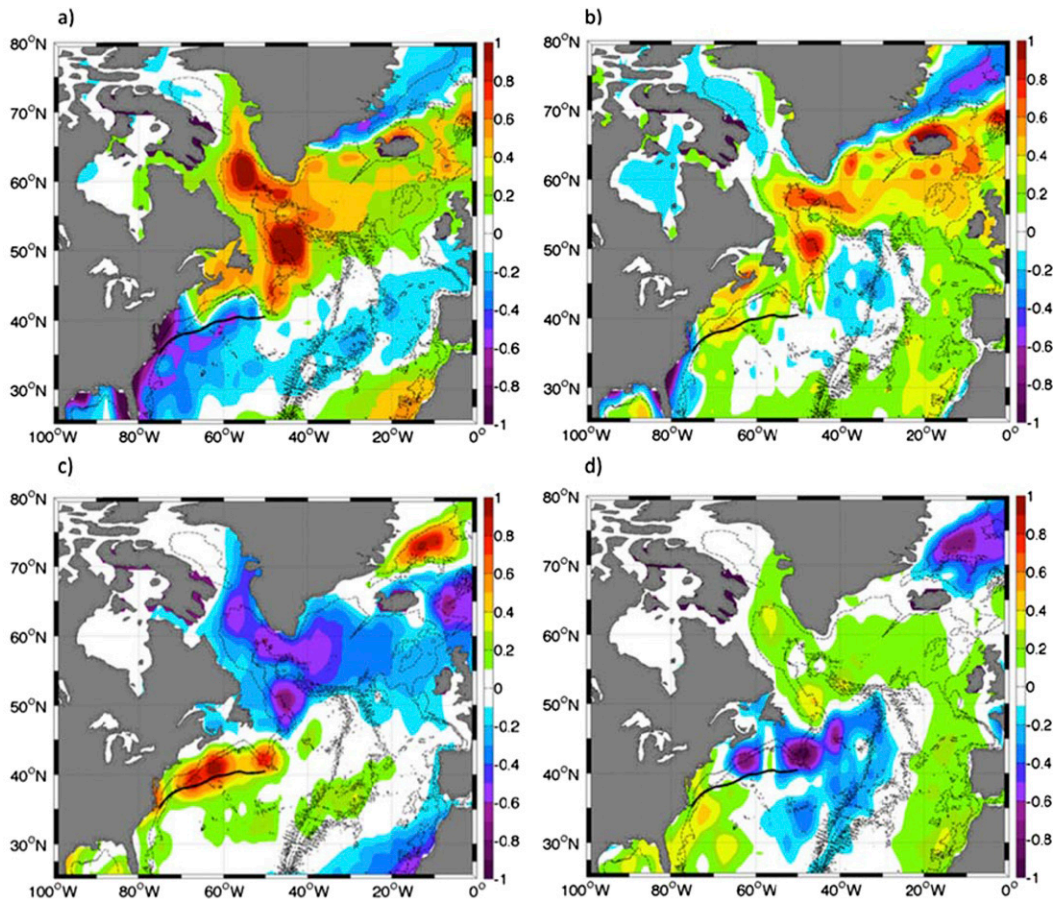


FIG. 2. Winter (DJF) composite SST anomalies ($^{\circ}\text{C}$) for the time range 1981–2012. Shown for the IL pressure during its highest years (a) with no lag and (b) with a 2-yr lag and the IL longitude during its easternmost years (c) with no lag and (d) with a 3-yr lag. The Gulf Stream path is superimposed (black line) on the SST anomalies. The thin lines represent the 1000- and 3500-m isobaths.

and conditions in the northeast Atlantic are milder, leading to the observed warm SST anomalies (Fig. 2a). Figure 2b shows SST anomalies for anomalously high IL pressure 2 years after those shown in Fig. 2a. The magnitude and the coverage of the warm SST anomalies are decreased (in comparison to Fig. 2a) in the Labrador Sea, east of Newfoundland, and in the Gulf of St. Lawrence and the Scotian Shelf. Further, comparing Fig. 1b with Fig. 2b, SSTs south of Grand Banks are found warmer in Fig. 1b (2 years after IL pressure was anomalously low) than in Fig. 2b (2 years after the IL pressure was anomalously high). This reduction in warm SSTs is suggestive of a displacement south in GSNW position.

Figure 2c presents SST anomalies for winters where the IL longitude was situated eastward by more than one standard deviation from its mean position (1983, 1984, 1994, 1995, 1999, and 2005). Warm SST anomalies dominate in a zonal band between the Mid-Atlantic Bight and just southeast of the Grand Banks, and strong

cool SST anomalies are observed in the Labrador Sea and south and east of Greenland (Fig. 2c). Similar to the anomalously high IL pressure conditions (Fig. 2a), anomalously east IL longitude (Fig. 2b) should depict warm SSTs in the general northeast Atlantic, opposite the pattern depicted during anomalously west IL longitudes (Fig. 1c). However, warm SSTs in Fig. 2b are only observed in the zonal band between the Mid-Atlantic Bight and the region southeast of the Grand Banks. The anomalously cool region in the Labrador Sea is unexplained and deserves further consideration. In Fig. 2d, 3 years after the IL longitude is at its easternmost, cool SST anomalies in the range of -0.3° to -1.0°C are observed in the neighborhood of the warm zonal band observed in Fig. 2c. The cooling of the SST anomalies near the Scotian Shelf and south of the Grand Banks 3 years after the IL longitude is at its easternmost (Fig. 2d) suggests a displacement south of the GSNW, just as warm anomalies in westernmost IL

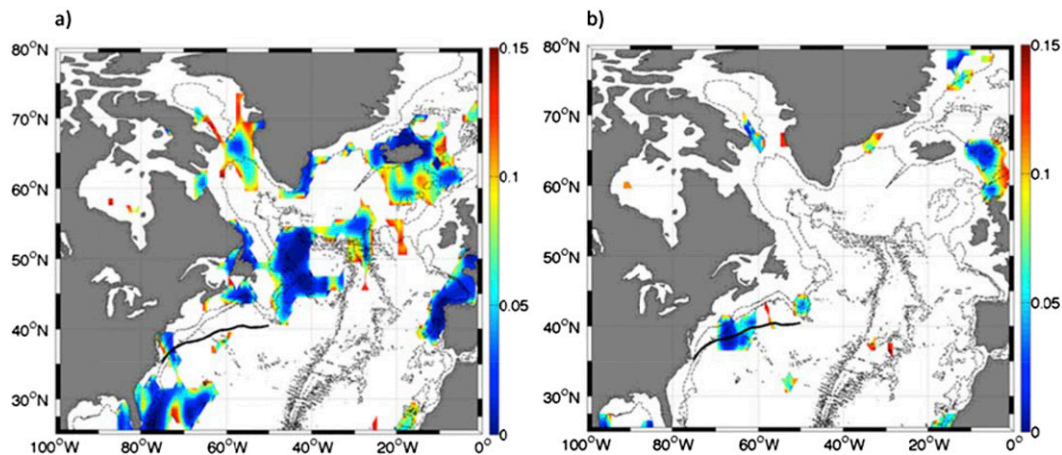


FIG. 3. (a) The p values of SST differences between winters during 1981–2012 in which IL pressure was anomalously low and winters in which IL pressure was anomalously high. (b) The p values of SST differences between winters in which IL was located anomalously westward and winters in which IL was located anomalously eastward. The black line represents the mean position of the Gulf Stream. The thin lines are the 1000- and 3500-m isobaths.

longitude, 3-yr lagged (Fig. 1d), suggest a northward shift in the GSNW.

Statistical significance of SST differences between the winters in which the IL pressure was anomalously low during the 1981–2012 period and the winters when the IL pressure was anomalously high are shown in Fig. 3a. This was carried out by doing a t test for the difference in the two mean temperatures at each grid point. Areas with p values less than 0.1 are seen in the Labrador Sea, south and east of Newfoundland, near the GSNW and in regions to the south. A similar test comparing winters in which the IL was situated anomalously west and anomalously east, shown in Fig. 3b, displays statistically significant differences near the GSNW and a small area in the Labrador Sea.

The impact of changes in the IL pressure can be seen in heat fluxes as well (Fig. 4). One-degree gridded net ocean surface heat flux data were used to make composites for winter (DJF) heat flux during anomalously low IL pressure years 1989, 1990, 1995, and 2007 (Fig. 4a) and during anomalously high IL pressure years 1996, 2001, 2004, and 2006 (Fig. 4b). The net heat flux (positive downward) used to construct these ensembles represents combined OAFlux and ISCCP products provided by the WHOI OAFlux project (<http://oafux.whoi.edu>) funded by the NOAA Climate Observations and Monitoring (COM) program, available from 1983 to 2009. The net heat flux Q_{net} is defined as

$$Q_{\text{net}} = \text{SW} - \text{LW} - \text{LH} - \text{SH},$$

where SW is the net downward shortwave radiation, LW is the net upward longwave radiation, LH is the latent heat flux, and SH is the sensible heat flux.

The composite net surface heat flux for anomalously low IL pressure years emphasizes negative heat flux in the Labrador and Greenland Seas as well as in the vicinity of the Gulf Stream (Fig. 4a). This negative heat flux has direct impact on mixed layer temperature and on deep convection. Heat flux for IL pressure during anomalously high pressure years (Fig. 4b) exhibits a similar pattern but with reduced magnitude in the Labrador and Greenland Seas, whereas negative heat flux in the Gulf Stream region has extended slightly south. Taking the difference between the IL low pressure years and IL high pressure years (Fig. 4c) shows the significantly stronger winter cooling in the Labrador and Greenland Seas ($\sim 50\text{--}80 \text{ W m}^{-2}$), which could lead to reduced mixed layer temperature and enhanced deep convection. These anomalies are markedly reduced over the Gulf Stream. For comparison, Fig. 4d shows the difference in winter SSTs between anomalously low IL pressure and anomalously high IL pressure years. Negative SST anomalies dominate the Labrador and Irminger Seas, the Scotian Shelf, and the Grand Banks (Fig. 4d). This pattern is similar to that observed in Fig. 4c, suggesting SST difference is linked to net heat flux changes. In general, comparison of Figs. 4c and 4d indicates that the intensified cooling in the subpolar gyre in IL low-pressure years spreads to large areas of the North Atlantic by ocean circulation.

5. Forecasting the GSNW position

Taylor and Stephens (1998) and Taylor et al. (1998) showed that the GSNW is autocorrelated with a lag of 1 year and correlated with the NAO and SOI, each with a 2-yr lag. Thus, it should be possible to forecast the

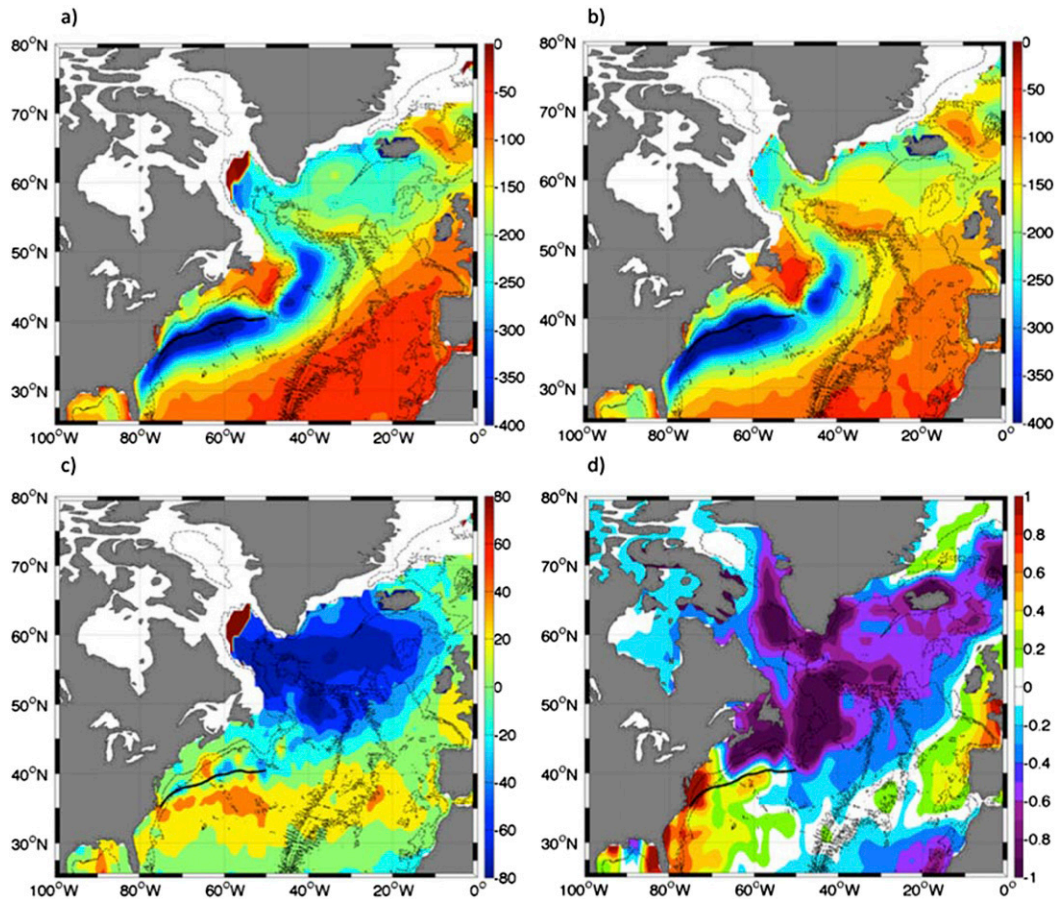


FIG. 4. Composite of net surface heat flux (positive downward) for (a) anomalously low IL pressure years and (b) anomalously high IL pressure years. (c) Difference in ensemble net surface heat flux between anomalously low and anomalously high IL pressure years and (d) difference in SST anomalies between anomalously low and anomalously high IL pressure. The units for net surface heat flux and SST are in W m^{-2} and degrees Celsius, respectively. The black line represents the mean position of the Gulf Stream. The thin lines are the 1000- and 3500-m isobaths.

GSNW at least 1 year ahead using these variables. A reliable scheme for predicting the GSNW should have practical value in view of the GSNW's known impact on plankton distribution in the North Atlantic.

Taylor and Gangopadhyay (2001) used the one-dimensional model developed by Behringer et al. (1979) to hindcast the interannual variations in the latitude of the GSNW. The model was forced by the monthly NAO index with a lag of 1 year. Based on the results presented in Table 1 and by Taylor and Stephens (1998) and Taylor et al. (1998), we developed a regression prediction model for the GSNW as

$$\text{GSNW}_i = a\text{GSNW}_{i-1} + b\text{ILP}_{i-2} + c\text{ILL}_{i-3} + d\text{SOI}_{i-2} + e,$$

where i represents a particular year and the subscripts of the independent variables represent the lag for each. The variables a , b , c , and d are regression coefficients

and e is the residual. In the first step, we developed a regression using the data from 1966 to 1993; the regression coefficients obtained were used to predict the GSNW index for 1994. Then, moving 1 year forward by developing a regression equation for 1966–94, we obtained a prediction for 1995, and so on until we had forecasts for each of the years during 1994–2015. In each of these calculations only prior information was used to make the prediction. These are 1-yr forecasts because the observed GSNW latitude from the previous year is used in predicting its value for the next year. In Fig. 5a, the solid line shows the observed values of the GSNW index and the dashed line shows the 1-yr-ahead predicted values. The amplitude of variations in the observations is underestimated by the predicted values. However, the maxima in the northward shifts of the GSNW in 1995, 2000, 2006, and 2009 are captured in the predicted values. Similarly, the extreme southward

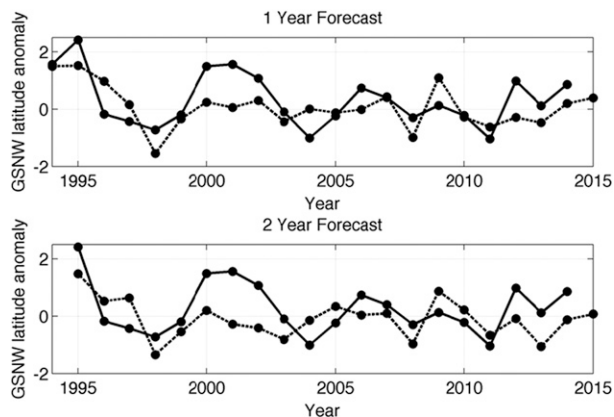


FIG. 5. Comparison of predicted (dashed lines) and observed (solid lines) GSNW position. (top) Forecasts made 1 year ahead and (b) forecasts made 2 years ahead.

shifts in 1998 and 2008 are reproduced in the predicted values. The correlation coefficient between the observed and forecasted values during 1994–2014 is 0.60 (significant at the 1% level) and the mean absolute error (MAE) is 0.53. We tested the stability of this prediction scheme by examining the values of R and MAE for four different durations. These are shown in Table 3, where it is seen that the correlation coefficient and the MAE were stable as the length of the forecast period increased. We note the MAE is defined here as

$$\text{MAE} = \frac{1}{n} \sum_{i=1}^n |f_i - y_i|,$$

where f_i is the predicted GSNW value and y_i is the observed GSNW value.

Table 4 gives the coefficients in the prediction model for the years 1994–2014. All variables were normalized to zero mean and unit standard deviation before computing the regressions. The table indicates that the IL pressure was the largest contributor to the forecasted value in the 1990s, but GSNW lagged 1 year was the largest contributor after the early 2000s. The contributions of IL longitude and the SOI fluctuated throughout this period.

The 2-yr-ahead forecasts were also made using the same scheme. For this purpose, we used the 1-yr forecasted value of the GSNW as a predictor in the regression equation. Comparison with the observed GSNW locations is shown in Fig. 5b. The 2-yr forecast also shows some skill. Correlation between the observed and forecasted values is 0.43 (slightly below the 5% significance level) and the MAE is 0.67; however, the 2-yr forecast is inferior to the 1-yr forecast in terms of both the correlation coefficient and the MAE. Both the 1- and 2-yr forecasts suggest that the annually averaged GSNW for

TABLE 3. Correlation coefficient R and the MAE during four segments of the forecast period. All correlations are significant at the 5% level.

	1994–2002	1994–2005	1994–2008	1994–2014
R	0.65	0.65	0.65	0.60
MAE	0.63	0.57	0.53	0.53

2015 will be slightly north of its value in 2014, as seen in Figs. 5a and 5b.

As a further check on consistency, cross correlations between GSNW and IL pressure during 1966–94, and then for each succeeding year until 2014, were also calculated (not shown here). The maximum correlation was found to be always with a lag of 2 years. A similar consistency was found in the correlation of GSNW with IL longitude being maximum at the lag of 3 years. However, the lag for maximum correlation between GSNW and the NAO index fluctuated between 1 and 2 years.

6. Conclusions

The results presented in this paper show that a forecast of the GSNW position, as given by Taylor and Stephens' (1998) GSNW index, is possible with a lead time of 1 year. The forecast uses only prior information on the following predictors: IL pressure (ILP; 2-yr lagged), the IL longitude (ILL; 3-yr lagged), the SOI (2-yr lagged), and the GSNW index (1-yr lagged). One-year forecasts of GSNW position were made for each of the years 1994–2015. Correlation between the forecasted and observed values for 1994–2014 was 0.60, significant at 1% level. The forecast for 2015 suggests that the annually averaged GSNW will be slightly north of its 2014 position. Forecasts of the GSNW index can have useful applications to fisheries as it has been shown to be related to variations of plankton in several regions of the North Atlantic.

Impact of IL pressure and its longitude on SST in the North Atlantic was also investigated. During years of anomalously low IL pressure, cool SSTs in the northern half of the North Atlantic subpolar gyre (specifically the region extending from the mouth of the Labrador Sea south to the Scotian Shelf and east toward the European continent) are observed (Fig. 1a). This SST structure is characteristic of an intensified IL pressure system, which leads to a reduced mixed layer temperature and enhanced deep winter convection in the Labrador and Greenland Seas region as shown by the negative heat flux patterns in Fig. 4a. The cool SSTs and increase in deep winter convection lead to warm SST anomalies south of the Grand Banks and east of the Scotian Shelf 2 years later (Fig. 1b). Similarly, during winters when the

TABLE 4. Coefficients of the prediction model. The columns list (left to right) the year for which the forecast is made; the coefficients of GSNW lagged 1 year, IL pressure (ILP) lagged 2 years, IL longitude (ILL) position lagged 3 years, and the SOI lagged 2 years; and the residual.

	GSNW _{<i>i</i>-1}	ILP _{<i>i</i>-2}	ILL _{<i>i</i>-3}	SOI _{<i>i</i>-2}	Residual
1994	0.35	-0.48	-0.32	-0.29	-0.15
1995	0.35	-0.48	-0.33	-0.29	-0.15
1996	0.40	-0.49	-0.35	-0.30	-0.11
1997	0.29	-0.53	-0.39	-0.30	-0.16
1998	0.30	-0.51	-0.42	-0.28	-0.17
1999	0.32	-0.48	-0.37	-0.29	-0.15
2000	0.31	-0.48	-0.38	-0.28	-0.14
2001	0.31	-0.46	-0.37	-0.35	-0.11
2002	0.38	-0.46	-0.34	-0.30	-0.06
2003	0.41	-0.46	-0.33	-0.28	-0.04
2004	0.43	-0.44	-0.32	-0.27	-0.03
2005	0.43	-0.43	-0.31	-0.28	-0.06
2006	0.44	-0.43	-0.31	-0.28	-0.06
2007	0.44	-0.42	-0.35	-0.26	-0.04
2008	0.44	-0.42	-0.35	-0.26	-0.04
2009	0.46	-0.38	-0.33	-0.26	-0.02
2010	0.48	-0.34	-0.29	-0.26	-0.04
2011	0.48	-0.34	-0.29	-0.26	-0.04
2012	0.48	-0.34	-0.29	-0.27	-0.05
2013	0.46	-0.33	-0.30	-0.30	-0.02
2014	0.48	-0.32	-0.31	-0.27	-0.02
Mean	0.40	-0.42	-0.33	-0.28	-0.07

IL longitude is anomalously west, cool SST anomalies are found in the Labrador Sea, east and south of Greenland, and south of the Grand Banks (Fig. 1c). Three years later, warm SST anomalies are perceived from the latitude of the Mid-Atlantic Bight to the Scotian Shelf and southeast of the Grand Banks (Fig. 1d). Both warm SST anomalies depicted in Figs. 1b and 1d suggest the GSNW experiences a northward shift 2 (3) years after the IL pressure (longitude) is anomalously low (west). This is likely due to a decrease in cool water sources to the slope sea, from the increased deep winter convection (Rossby and Benway 2000).

Conversely, during years of anomalously high IL pressure, warm SSTs permeate the Labrador Sea, the Gulf of St. Lawrence, the Scotian Shelf, and the Grand Banks (Fig. 2a), and during anomalously east IL longitude, warm SSTs extend zonally from the Mid-Atlantic Bight to the region southeast of the Grand Banks (Fig. 2c). The SST anomaly signal for anomalously high IL pressure is as expected for the milder cyclonic conditions that accompany the weakened IL pressure system [with the exception of the cool SST anomalies observed in the Labrador Sea (Fig. 2c), which are unexplained here and deserve further consideration]. At the same time, the composite of net surface heat flux during winters where IL pressure was anomalously high show a decrease in net surface heat flux in the Labrador

and Greenland Seas region (Fig. 4b), suggesting a decrease in deep winter convection. Two (three) years after the anomalously high (east) IL pressure (longitude), SST anomalies have cooled (Figs. 2 b,d) relative to Figs. 2a and 2c, suggesting a displacement south in GSNW position. Further, the difference in net surface heat flux between years when the IL pressure was anomalously low and years when it was anomalously high was considered (Fig. 4c) and compared to the SST anomalies for the IL low-pressure and IL high-pressure years (Fig. 4d). Figure 4c emphasized significantly stronger winter signal in the Labrador and Irminger Seas and reduced heat fluxes over the Gulf Stream region, similar to the strong SST anomaly signal observed in Fig. 4d. These results suggest changes in ocean temperatures in the subpolar gyre induced by the IL can be attributed to changes in heat fluxes as well as those due to wind stress changes.

We note lags of 2 years for the IL pressure and 3 years for its longitude position were used in the calculations in this paper. However, lags between changes in the IL and the GSNW can vary over a range of years as shown in Table 3 and are to be expected from the variable nature of processes in the atmosphere and the ocean.

Acknowledgments. We thank C. N. Flagg for his feedback and comments on the earlier versions of this work as well as three anonymous reviewers. This research was partly supported by the grants NSF OCE-0825418 and OCE-1060752.

REFERENCES

- Bane, J. M., Jr., O. B. Brown, R. H. Evans, and P. Hamilton, 1988: Gulf Stream remote forcing of shelfbreak currents in the Mid-Atlantic Bight. *Geophys. Res. Lett.*, **15**, 405–407, doi:10.1029/GL015i005p00405.
- Behringer, D., L. Regier, and H. Stommel, 1979: Thermal feedback on wind-stress as a contributing cause of the Gulf Stream. *J. Mar. Res.*, **37**, 699–709.
- Borkman, D. G., and T. J. Smayda, 2009: Gulf Stream position and winter NAO as drivers of long-term variations in the bloom phenology of the diatom *Skeletonema costatum* “species-complex” in Narragansett Bay, RI, USA. *J. Plankton Res.*, **31**, 1407–1425, doi:10.1093/plankt/fbp072.
- Bower, A. S., and H. D. Hunt, 2000: Lagrangian observations of the deep western boundary current in the North Atlantic Ocean. Part I: Large-scale pathways and spreading rates. *J. Phys. Oceanogr.*, **30**, 764–783, doi:10.1175/1520-0485(2000)030<0764:LOOTDW>2.0.CO;2.
- Csanady, G.T., and P. Hamilton, 1988: Circulation of slope water. *Cont. Shelf Res.*, **8**, 565–624, doi:10.1016/0278-4343(88)90068-4.
- Hameed, S., and S. Piontkovski, 2004: The dominant influence of the Icelandic Low on the position of the Gulf Stream northwall. *Geophys. Res. Lett.*, **31**, L09303, doi:10.1029/2004GL019561.
- Han, G., K. Ohashi, N. Chen, P. G. Myers, N. Nunes, and J. Fischer, 2010: Decline and partial rebound of the Labrador Current 1993–2004: Monitoring ocean currents from altimetric and conductivity-temperature-depth data. *J. Geophys. Res.*, **115**, C12012, doi:10.1029/2009JC006091.

- Jennings, E., and N. Allott, 2006: Position of the Gulf Stream influences lake nitrate concentrations in SW Ireland. *Aquat. Sci.*, **68**, 482–489, doi:[10.1007/s00027-006-0847-0](https://doi.org/10.1007/s00027-006-0847-0).
- Kalnay, E., and Coauthors, 1996: The NCEP/NCAR 40-Year Reanalysis Project. *Bull. Amer. Meteor. Soc.*, **77**, 437–471, doi:[10.1175/1520-0477\(1996\)077<0437:TNYRP>2.0.CO;2](https://doi.org/10.1175/1520-0477(1996)077<0437:TNYRP>2.0.CO;2).
- Pickart, R. S., and W. M. Smethie, 1993: How does the deep western boundary current cross the Gulf Stream? *J. Phys. Oceanogr.*, **23**, 2602–2616, doi:[10.1175/1520-0485\(1993\)023<2602:HDTDWB>2.0.CO;2](https://doi.org/10.1175/1520-0485(1993)023<2602:HDTDWB>2.0.CO;2).
- Planque, B., and A. H. Taylor, 1998: Long-term changes in zooplankton and the climate of the North Atlantic. *J. Mar. Sci.*, **55**, 644–654.
- Quenouille, M. H., 1953: *Associated Measurements*. Butterworth Scientific, 241 pp.
- Rossby, T., and R. Benway, 2000: Slow variations in mean path of the Gulf Stream east of Cape Hatteras. *Geophys. Res. Lett.*, **27**, 117–120, doi:[10.1029/1999GL002356](https://doi.org/10.1029/1999GL002356).
- Taylor, A. H., 1995: North–south shifts of the Gulf Stream and their climatic connection with the abundance of zooplankton in the UK and its surrounding areas. *ICES J. Mar. Sci.*, **52**, 711–721, doi:[10.1016/1054-3139\(95\)80084-0](https://doi.org/10.1016/1054-3139(95)80084-0).
- , and J. A. Stephens, 1980: Latitudinal displacements of the Gulf Stream (1966 to 1977) and their relation to changes in temperature and zooplankton abundance in the NE Atlantic. *Oceanol. Acta*, **3** (2), 145–149.
- , and —, 1998: The North Atlantic Oscillation and the latitude of the Gulf Stream. *Tellus*, **50A**, 134–142, doi:[10.1034/j.1600-0870.1998.00010.x](https://doi.org/10.1034/j.1600-0870.1998.00010.x).
- , and A. Gangopadhyay, 2001: A simple model of interannual displacements of the Gulf Stream. *J. Geophys. Res.*, **106**, 13 849–13 860, doi:[10.1029/1999JC000147](https://doi.org/10.1029/1999JC000147).
- , M. B. Jordan, and J. A. Stephens, 1998: Gulf Stream shifts following ENSO events. *Nature*, **393**, 638, doi:[10.1038/31380](https://doi.org/10.1038/31380).